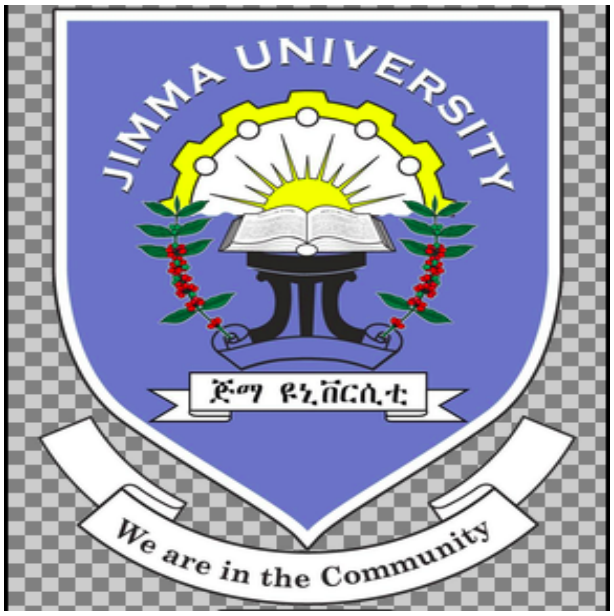

GLOW CURVE DECONVOLUTION ANALYSIS OF CALCIUM MAGNESIUM SILICATE NANOPHOSPHOR

A THESIS SUBMITTED TO The Department OF PHYSICS PRESENTED IN PARTIAL FULFILLMENT OF THE REQUIREMENTS FOR THE DEGREE OF MASTER OF SCIENCE IN PHYSICS

(**CONDENSED MATTER PHYSICS**)

By

ITIYANE LEGESE

ADVISOR:- **NEBIYU GEMECHU (PhD)**

JIMMA, ETHIOPIA

AUGUST, 2022

Approval Sheet

SCHOOL OF GRADUATE STUDIES

JIMMA UNIVERSITY

COLLEGE OF NATURAL SCIENCES

MSc. THESIS APPROVAL SHEET

We undersigned number of the Board of Examiners of the final open defense by Itiyane Legese have read and evaluated her thesis entitled "Glow Curve Deconvolution Analysis Of Calcium Magnesium Silicate Nanophosphor" and examined the candidate. This is therefore to certify that the thesis has been accepted in partial fulfillment of the requirements for the degree Master of Science in Physics (Condensed Matter Physics).

Chair person :————————————————————————-

Signature ———————————— date ————————————-

Advisor : Dr.Nebiyu Gemechu

Signature ———————————— date————————————

External Examiner :————————————————————————-

Signature————————--date————————————

Internal Examiner:————————————————————————

Signature ———————————— date————————————

SCHOOL OF GRADUATE STUDIES

JIMMA UNIVERSITY

Date : July 2022

Author : **Itiyane Legese**

Title : **Glow Curve Deconvolution Analysis Of Calcium Magnesium Silicate Nanophosphor**

Department : **Physics**

Degree : **M.Sc.** Convocation : **July** Year : **2022**

Permission is herewith granted to Jimma University to circulate and to have copied for non-commercial purposes, at its discretion, the above title upon the request of individuals or institutions.

_____

Signature of Author

Contents

List of Figures

List of Tables

Abstract

Thermoluminescence(TL) is a luminescence phenomenon of an insulator or semiconductor which can be observed when the solid is thermally stimulated. The glow curve deconvolution(GCD) is mainly used to find the individual glow peaks of a composite TL Glow curve and further to evaluate the trapping parameters. The purpose of this research was to analyze glow curve of calcium magnesium silicate nanophosphor and deconvolute the curve in to its individual peaks using Origin software and this was based on the concept of one trap-one recombination center(OTOR) model. Four peaks were deconvoluted and we determined activation energy(E) and frequency factor(s) for each peak using peak shape method. With the determined values of activation energy(E) and frequency factor(s) the graph of concentration of electron(n(T)) and TL intensity versus temperature was plotted in Mathematica. And we observed that the value of maximum temperature experimentally and calculated were close to each other for these peaks. Also, shift of TL intensity of these peaks were observed.

Acknowledgment

First of all I would like to thank the almighty God, my strength, power and leading me to this position. I would like to express my deepest gratitude to my advisor Dr. Nebiyu Gemechu for his valuable, and constructive suggestion starting from the planning up to the development of this thesis work. I thank him a lot for his guidance to the right research direction. Next, I would like to thank my co-advisor Dr. Menbaru.M for his insightful comment to the accuracy of this thesis, continuous encouragement during my proposal delivery up to the final of this thesis. Next I thank my husband Lencho Kajela for motivating and strengthening me to carry out this project. Last but not least, I would also extend my sincere thanks to my all family, for their moral support.

1

Introduction

1.1 Back ground of the study

Luminescence is defined as the emission of light above that expected for black body, from some solids commonly called phosphors. This emission is the release of energy stored within the solid through some type of prior excitation of the solid electronic system, i.e.,by visible, infrared (IR) or ultra violet (UV) light and ionizing radiation. The ability to store the radiation energy is important in luminescence dosimetery and is generally associated with the presence of activators which act as trapping levels for the free electrons generated by excitation. Where the activators are impurity atoms and structural defects[13]. Thermoluminescence(TL) is a luminescence phenomenon of an insulator or semiconductor which can be observed when the solid is thermally stimulated. TL should not be confused with the light spontaneously emitted from a substance when it is heated to incandescence. At higher temperatures (in excess of 200°C) a solid emits (infra) red radiation of which the intensity increases with increasing temperature. This is thermal or black body radiation. TL, however, is the thermally stimulated emission of light following the previous absorption of energy from radiation. There are three essential ingredients necessary for the production of TL. Firstly, the material must be an insulator or a semiconductor[23]. But metals do not exhibit luminescent properties because they could not storage radiation energy[32]. Secondly, the material must have at some time absorbed energy during exposure to ionizing radiation.

The stored energy is released in the form of visible light when the material is heated. Thirdly, the luminescence emission is triggered by heating the material[23]. The well known model for explaining a single thermoluminescence (TL) peak consists of an electron trapping state, the conduction band and a hole center[9]. In TL, thermal energy is used to release trapped electrons from their traps to the conduction band. Upon minimizing the internal energy the free electrons migrate from the conduction band to lower energy states. This transition may be radiative which causes the glow observed from the material. According to the OTOR model, this radiative transition results in the formation of a glow curve composing of a single peak[17]. Glow curve deconvolution(GCD) is mainly used to find the individual glow peaks of a composite TL glow curve and further to evaluate the trapping parameters E(activation energy) and s(frequency factor)[21].

Aluminate-based rare earth-ion-doped phosphors have attracted a great deal of interest because of their excellent properties, e.g., high brightness, long duration, excellent photo-resistance and environmental capability. However, the properties of these phosphors are decreased greatly on soaking in water for several hours, which limits their application[6]. Recently, silicate-based phosphors have attracted much attention because of their many advantages over sulfide and aluminate phosphors([11],[15],[33]), such as: high thermal and chemical stability, water resistance, quantum yield of up to 70% and high radiation intensity. These features come from the weak interaction between the matrix and the activator ion, so the excitation and emission spectra are determined mostly by the nature of the activator ion. Besides, these hosts have a wide band gap and absorb in the far UV-region[1]. Some of the compounds existing in the Ca-Mg-Si-O system include diopside($CaMgSiO_4$), bredigite($Ca_7MgSi_4O_{16}$) akermanite($Ca_2MgSi_2O_7$), merwinite(Ca_3MgSiO_8) and monticelite($CaMgSiO_4$)([22],[10]).

1.2 Statement of the Problem

The glow curve measured from TL materials looks complicated due to the existence of multi-electron and hole traps. In the One Trap One Recombination model, the measured glow curve is considered to be produced by summing up individual glow peaks. To analyze the obtained glow curve, Computerized glow-curve deconvolution is the most used method. This study was designed to analyze glow curve using Origin software and to determine the kinetic parameters: trap depth or activation energy(E) and frequency factor(s) for all deconvoluted peaks from the glow curve of host material calcium magnesium silicate nanophosphor($CaMgO_4Si$) using peak shape method.

1.3 Research Question

The research questions of the study were:

- how many glow peaks we will obtain from the glow curve deconvolution analysis of $CaMgO_4Si$?
- what is the value of activation energy(E) and frequency factor of the deconvoluted peaks of Calcium Magnesium Silicate nanophosphor($CaMgO_4Si$)?

1.4 Objectives

1.4.1 General objective

The main objective of the study was glow curve deconvolution analysis of Calcium Magnesium Silicate nanophosphor.

1.4.2 Specific objectives

The specific objective of the study were:

- to analyze glow peaks of Calcium Magnesium Silicate nanophosphor($CaMgO_4Si$).
- to determine trap parameters: activation energy(E) and frequency factor(s) for the deconvoluted glow peaks of $CaMgO_4Si$.

1.5 Limitation of the Study

The research study was not free from limitation. Here are some limitations like,

- Lack of references on the title.
- Shortage of time.
- Lack of internet access.

1.6 Scope of the Study

The scope of the study was limited to analyzing glow curve of calcium magnesium silicate nanophosphor, deconvolting the peaks on Origin software and determining activation energy and frequency factor for the deconvoluted peaks using peak shape method. Therefore, the study was only focused on the explanation of glow curve deconvolution analysis of calcium magnesium silicate nanophosphor and calculating trap depth(E) and frequency factor(s) from the deconvoluted glow peaks.

2

Review of Related Literature

2.1 Luminescence

Luminescence is "cold light", light from other sources of energy, which can take place at normal and lower temperatures. The materials exhibiting this phenomenon are known as 'Luminescent materials' or 'Phosphors' meaning 'light bearer' in Greek. Solids exhibiting property of luminescence are usually referred to as Phosphors. In luminescence, some energy source kicks an electron of an atom out of its "ground" (lowest energy) state into an "excited" (higher-energy) state. Then the electron gives back the energy in the form of light in the visible region, so that it can fall back to its "ground" state. In the process of luminescence, when radiation is incident on a material some of its energy is absorbed and re-emitted as a light of a longer wavelength (Stokes law). Wavelength of light emitted is characteristic of a luminescent substance and not of the incident radiation. This cold emission, involves two steps:[24]

1. The excitation of electronic system of a solid material to higher energy state,
2. Subsequent emission of photons or simply light.

2.1.1 Types of Luminesence

There are several varieties of luminescence each named according to what the trigger for the luminescence is[24]:

- **Chemiluminescence**: is the emission of light by the release of energy from a chemical reaction.

- **Bioluminescence**: is produced by biological processes. Is also known as "living light" and the most amazing examples of this phenomenon can be found in the deep seas.
- **Triboluminescence or Mechanoluminescence**: is type of luminescence which is generated by mechanical energy.
- **Cathodoluminescence**: the emission light is a result of electron beam excitation.
- **Electroluminescence**: light is generated in response to an applied electric field on a certain material.
- **Photoluminescence**: emission of the light is the result of the excitation by electromagnetic radiation or photons.
- **Thermoluminescence**: is the luminescence activated thermally after initial irradiation by other means such as α, β, γ, UV or X-rays.
- **Radioluminescence**: it is the phenomenon by which light is produced in a material by bombardment with ionizing radiation such as beta particles, X-rays or gamma rays.
- **Sonoluminescence**: is produced due to the excitation by ultrasonic waves[24] or produced by high frequency sound waves or phonons.

2.2 Thermoluminescence

Thermoluminescence is observed in the process of irradiating a material, when part of the irradiation energy is used to transfer electrons to traps. It is also known as thermally stimulated luminescence (TSL). This energy, stored in the form of the trapped electrons, is released by raising the temperature of the material, and the released energy is converted to luminescence. Information of the trapping process and the release of trapped electrons is obtained from the thermoluminescence(TL) spectrum. The shape and position of the resultant TL glow curves can be analyzed to extract information on the various parameters of the trapping process—trap depth, trapping and re-trapping rates[4].

2.3 Trap Parameters

In the study of thermoluminescence(TL), one may be interested in the values of the relevant trapping parameters. These parameters and the relation between them are of importance in determining the temperatures of the TL peaks[8]. There are so many trap parameters in the process of Thermoluminescence. From these activation energy(E), frequency factor(s) and order of kinetics are the main one. In glow curve deconvolution analysis they are determined from each individual glow peaks.

2.3.1 Activation Energy(E)

It is the energy expressed in eV, assigned to a metastable state or level within the forbidden gap between the conduction band and valence band of a crystal.This energy is also called trap depth. The metastable level can be an electron trap near to the conduction band, or hole trap near to valence band(or luminescence center). The metastable is originated by defects of the crystal structure. Bombarding the solid with an ionizing radiation, this produces free charges which can be trapped at the metstable states[12]. Supposing the solid previously heated, a quantity of energy supplied in the form of thermal energy required to release thermally a trapped electron into the conduction band([12],[8]). For an electron trap, E is measured in eV, from the trap level to the bottom of the conduction band. For a hole trap, E is measured from the trap to the top of the valence band[12].

2.3.2 Frequency Factor(s)

The frequency factor s, is known as attempt to escape frequency. The frequency factor $s(s^{-1})$ should be of the order of magnitude of the Debye frequency $(10^{12} - 10^{14}s^{-1})$. This parameter is proportional to the frequency of the collisions of the electron with the lattice phonons[25]. According to chen, the possible range for s is $(10^{5} - 10^{13}s^{-1})$[7].

2.3.3 Order Of Kinetics

The equations governing the thermoluminescence processes have been given by Randall–Wilkins, Garlick–Gibson and May–Partridge for first order, second order and

general order respectively[25].

For first order

$$I(t) = -\frac{dn}{dt} = nse^{-E/kT} \tag{2.1}$$

For second order

$$I(t) = -\frac{dn}{dt} = \frac{n^2}{N}se^{-E/kT} \tag{2.2}$$

For general order

$$I(t) = -\frac{dn}{dt} = n^b s^{'} e^{-E/kT} \tag{2.3}$$

Where:

- s is a constant characteristic of the electron trap, called the "preexponential frequency factor" or "attempt-to-escape frequency" (s^{-1}).
- N is the total trap concentration(m^{-3}).
- n is the concentration of trapped electrons at time $t(m^{-3})$.
- b is the kinetic order, a parameter with values typically between 1 and 2.
- $s^{'}$ = the effective pre-exponential factor for general order kinetics $(m^{3(b-1)}s^{-1})$.

2.4 Model Of Thermoluminescence

From a theoretical point of view, TL is directly connected to the band structure of solids and particularly to the effects of impurities and lattice irregularities. It is useful to describe the band structure in term of valence and conduction bands, parted from each other by a forbidden gap in which the defects are represented. The mapping of the forbidden gap reveals quite a complex configuration, and the experimental TL emission study can provide a satisfactory tool to get detailed information on its most important parameters. The most promising tool is the observation and the recording of TL emission as a function of temperature at which the TL sample is heated[14].

2.4.1 One Trap One Recombination model(OTOR)

The simplest model to explain thermoluminescence process is OTOR model.

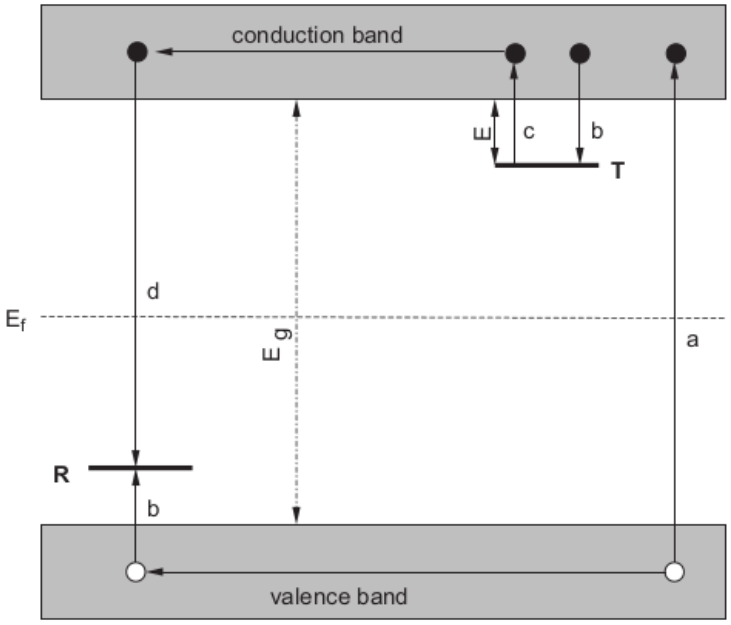

Figure 2.1: One Trap One Recombination model(OTOR)

Where:

- (a) generation of electrons and holes
- (b) electron and hole trapping
- (c) electron release due to thermal stimulation
- (d) recombination
- Solid circles are electrons, open circles are holes
- Level T is a electron trap
- level R is a recombination centre
- E_f is Fermi level and
- E_g is the energy band gap.

The conduction band separated from the valence band by the so-called forbidden band gap. However, if there are impurities within the lattice, there is a possibility for electrons to possess energies which are forbidden in the perfect crystal. In a simple TL model two levels are assumed, one situated below the bottom of the conduction band and the other situated above the top of the valence band (see Fig 2.1). The highest level indicated by T is situated above the equilibrium Fermi level(E_f) at equilibrium state, i.e. before the exposure to radiation and the creation of electrons and holes. The other level (indicated by R) is a potential hole trap and can function as a recombination center. The absorption of radiant energy with $h\nu > E_g$results in ionization of valence electrons, producing energetic electrons and holes which will, after thermalisation, produce free electrons in the conduction band and free holes in the valence band (transition a). The free charge carriers recombine with each other or become trapped.

In the case of direct recombination an amount of energy will be released which may excite a luminescent center. The luminescent center returns to the ground state under the emission of light. However, in insulators and semiconductors a certain percentage of the charge carriers is trapped: the electrons at T and the holes at R (transition b). The probability unit time of release of an electron from the trap is assumed to be described by the Arrhenius equation:

$$P = s \exp\{\frac{-E}{kT}\} \tag{2.4}$$

where:

- p is the probability per unit time.
- s is the frequency factor(temperature independent) or attempt to escape factor, with a value in the order of the lattice vibration frequency $10^{12}, 10^{14} s^{-1}$.
- E is called the trap depth or activation energy, the energy needed to release an electron from the trap into the conduction band[5].

In the simple model this recombination center is a luminescent center where the recombination of the electron and hole leaves the center in one of the higher excited

states. Return to the ground state is coupled with the emission of light quanta(i.e. thermoluminescence). The intensity of TL I(t) in photons per second at any time t during heating is proportional to the rate of recombination of holes and electrons at R, can be written as:

$$I(t) = -\frac{dm}{dt} \tag{2.5}$$

Negative sign indicates a decrease of holes and 'm' is the concentration of holes trapped at R. equation[25]:

$$\ln[I_M^{b-1}(\frac{T_m^2}{\beta})^b] = \frac{E}{kT_m} + c \tag{2.6}$$

where c is constant. Using Eq. (3.8), it is possible to evaluate the quantity on the left-side for different values of b, and to obtain a set of graphs as a function of $1/(kT_m)$. The value of b for which the graph best approximates linearity is found, and the graphs are fitted by a straight line whose slope is E. The method is valid for general heating rates, i.e., the heating rate β does not need to be constant. For the case of second-order kinetics (b = 2), Eq. (3.8) becomes

$$\ln[I_m(\frac{T_m^2}{\beta})^2] = \frac{E}{kT_m} + c \tag{2.7}$$

This method is useful only when b is appreciably different from unity, since for b = 1 the temperature T_m of maximum TL intensity is independent of the initial concentration n_o of trapped electron.

2.5 Applications of Calcium Magnesium Silicate Nanophosphor

Calcium Magnesium Silicate Nanophosphor has so many applications. For example,

- **Diopside (**$CaMgSi_2O_6$**)**: is one of the pyroxene minerals, is known as an excellent bioactive material[18]. Diopside finds use in a wide variety of clinical applications such as bone and dental root implants, surgery hemostasis applications, drug delivery and in vivo imaging[30]. In addition, the sintered body of diopside seems to

bond to living bone tissues more rapidly than apatite. It has a fairly high mechanical strength and super biological affinity. Diopside is therefore considered to have a potential as a biomaterial for artificial bone and tooth[18].

- **Akermanite(**$Ca_2MgSi_2O_7$**)**: as a bioactive silicate ceramic has received considerable attention due to its highly controllable mechanical properties, biodegradation, and bioactivity. It could be employed as an efficient bioactive ceramic for bone reconstruction, surface coating of implants, and angiogenic applications[29].

- **Bredigite(**$Ca_7MgSi_4O_{16}$**)**: is a bioactive ceramic that possesses apatite-formation ability. Natural human bone is composed of nanostructured apatite in collagen matrix. To provide a good coating for the implants, it is best if the coating material is similar to bone minerals in crystal structure, size and morphology[28].

3

Materials and Methods

3.1 Materials

The sources of information for this thesis were the published articles, books and dissertation based on the thesis title. And types of Software's used for the preparation of the thesis were latex for writing, Origin software for analyzing the glow curve and deconvoluting the peaks, and Wolfram mathematica for plotting the graph of concentration of electron and TL intensity versus temperature.

3.2 Method

We studied Glow curve deconvolution analysis of Calcium Magnesium Silicate Nanophosphor. First of all the experimental data of the host material was plotted on the Origin software. The Glow curve was analyzed and peaks were deconvoluted. By using Anotation command in the Origin software, the parameters(I_M, $I_M/2$, T_M, T_1 and T_2) were extracted from the peaks and recorded in the table. From different methods of analysis of TL Glow curve, the peak shape method was used to determine activation energy(E) using the following equation:

$$E_\alpha = C_\alpha(\frac{kT_M^2}{\alpha}) - b_\alpha(2kT_M) \tag{3.1}$$

where,

$\alpha = \tau$

$$C_\tau = 1.51 + 3.0(\mu_g - 0.42) \ \ and \ \ b_\tau = 1.58 + 4.2(\mu_g - 0.42) \tag{3.2}$$

α = δ

$$C_\delta = 0.976 + 7.3(\mu_g - 0.42) \ \ and \ \ b_\delta = 0 \tag{3.3}$$

α = ω

$$C_\omega = 2.52 + 10.2(\mu_g - 0.42) \ \ and \ \ b_\omega = 1.0 \tag{3.4}$$

And once the value of activation energy determined frequency factor can be calculated by Kitis et al equation[25] of second order peak.

$$s = \frac{\beta E}{kT_M^2(1 + \frac{2kT_M}{E})} \exp(\frac{E}{kT_M}) \tag{3.5}$$

Finally, the graph of concentration of electron and TL intensity versus temperature were plotted on the Mathematica software.

4

Results and Discussions

In this chapter, we seek to determine the activation energy E and frequency factor s, for all deconvoluted peaks from the original curve of host material($CaMgO_4Si$) by employing the peak shape(Chen's peak shape) method using the values of I_m, T_m, T_1 and T_2 which extracted from the deconvoluted peaks using origin software. We got the original curve from the experimental data.

4.1 Analysis of Glow Curve from Experimental Data

We got the glow curve on the left side(the black one) from the experimental data by using origin software. The curve on the right side was the deconvoluted peaks from the original curve. About four peaks were deconvoluted(see 4.1). For each peaks the parameters($I_m, T_m, T_1 and T_2$) were extracted by using (Anotation) in the origin(see Table 4.1). For more understanding, the picture of each peak is given separately in fig. 4.2.

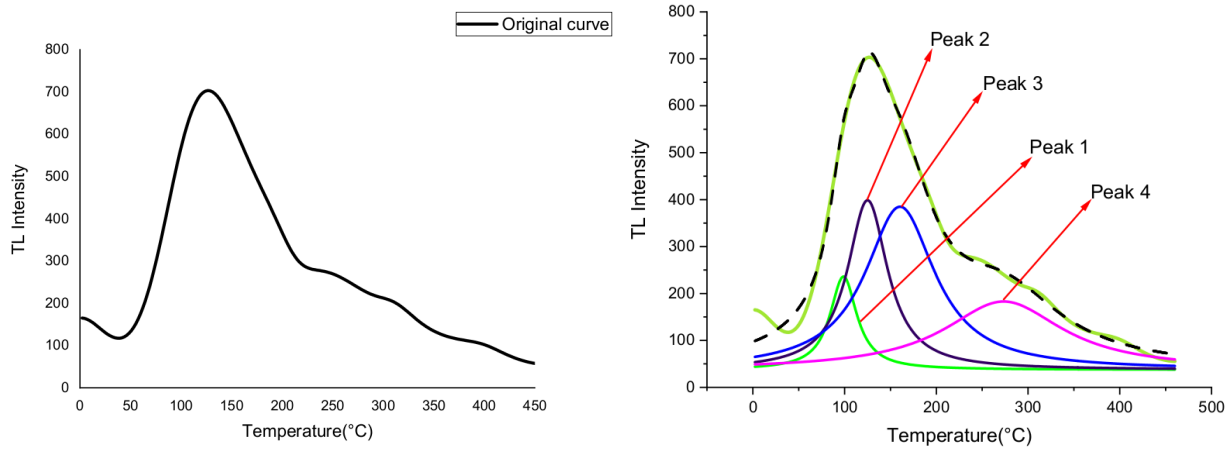

Figure 4.1: Original curve from the experimental data and the deconvoluted peaks

4.2 Calculation of Activation Energy(E) and Frequency factor(s)

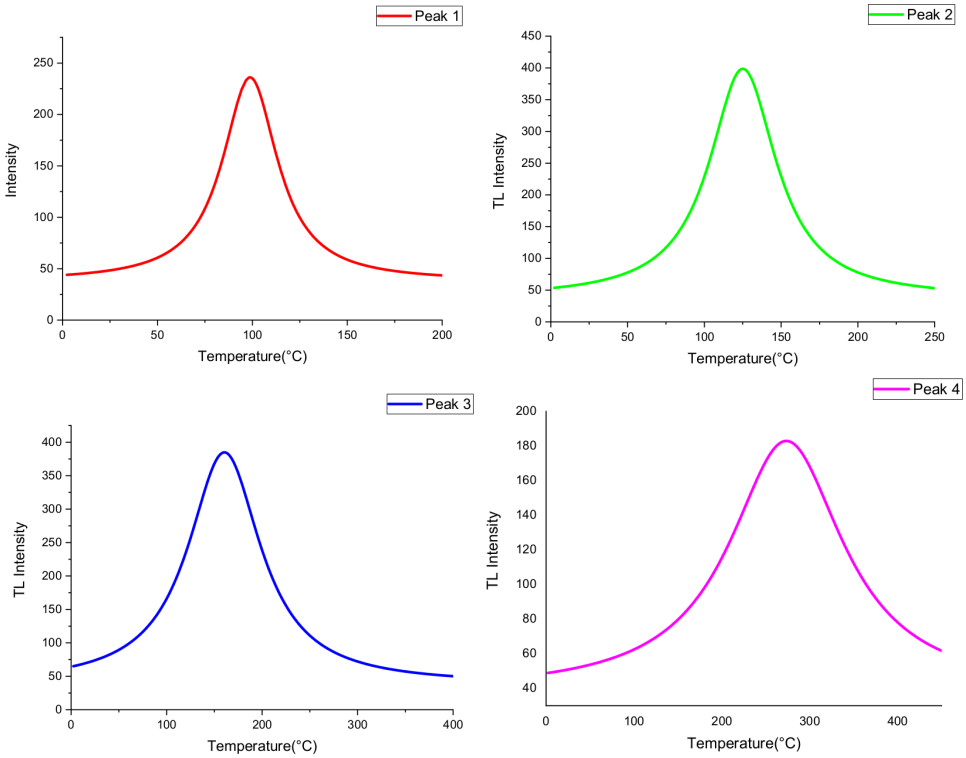

Figure 4.2: The four deconvoluted peaks separately

Peaks	I_M	$I_M/2$	T_M(°C)	T_1(°C)	T_2(°C)	T_M(K)	T_1(K)	T_2(K)
Peak 1	236.1	118.1	98.9	78.2	120.05	371.9	351.2	393.05
Peak 2	398.59	199.3	125.09	96.6	154.1	398.09	369.6	427.1
Peak 3	384.94	192.5	160.37	109.051	212.31	433.37	382.05	485.31
Peak 4	182.9	91.5	273.53	170.2	376.156	546.53	443.2	649.5

Table 4.1: Values of Intensity and Temperature for each peaks

The main goal of measuring and analyzing these TL glow curves is the extraction of several parameters that can be used to describe the TL process in the material. Among the important TL parameters are the activation energy (E) and the frequency factor. Below, employing the data extracted from Figs. 4.2 and displayed in Tables 4.1 the two parameters are computed using the methods peak shape method(Chen's peak shape method) discussed in chapter 3 for each peaks. According to Chen's peak shape method We have first calculate the geometrical shape quantities $\mu, \tau, \delta, and \omega$. Where,

$\tau = T_M - T_1$

$\delta = T_2 - T_M$

$\omega = T_2 - T_1$

$\mu = \frac{\delta}{\omega}$

4.2.1 Activation Energy(E)

Peaks	τ	δ	ω	μ
Peak 1	20.7	21.15	41.85	0.51
Peak 2	28.49	29.01	57.5	0.5
Peak 3	51.32	51.49	103.26	0.5
Peak 4	103.33	102.97	206.3	0.5

Table 4.2: The values of geometrical shape quantities for each peak

The values of μ for each peak were given in the table above(table 4.2) and these values were very close to the value μ for second order kinetics, which is μ=0.52. So, to determine the activation energy(E) for both peaks, the peak shape method expression of second order kinetics was used.

peak 1

using the value of τ = 20.7:

$$E = \frac{1.81kT_M^2}{\tau} - 2(2kT_m) \tag{4.1}$$

$$E = \frac{1.81 * 8.617 * 10^{-5}(371.9)^2}{20.7} - 2(2 * 8.617 * 10^{-5} * 371.9) \tag{4.2}$$

$$E = 1.04eV - 0.13eV = \underline{0.91eV} \tag{4.3}$$

where, $k = 8.617 * 10^{-5} eV K^{-1}$

using the value of δ:

$$E = \frac{1.71kT_M^2}{\delta} \tag{4.4}$$

$$E = \frac{1.71 * 8.617 * 10^{-5}(371.9)^2}{21.15} \tag{4.5}$$

$$E = \underline{0.96eV} \tag{4.6}$$

using the value of ω:

$$E = \frac{3.54kT_M^2}{\omega} - 2kT_M \tag{4.7}$$

$$E = \frac{3.54 * 8.617 * 10^{-5}(371.9)^2}{41.85} - 2 * 8.617 * 10^{-5} * 371.9 \tag{4.8}$$

$$E = 1.01eV - 0.06eV = \underline{0.95eV} \tag{4.9}$$

Peak 2

using the value of τ

$$E = \frac{1.81kT_M^2}{\tau} - 2(2kT_M) \tag{4.10}$$

$$E = \frac{1.81 * 8.617 * 10^{-5}(398.09)^2}{28.49} - 2(2 * 8.617 * 10^{-5} * 398.09) \tag{4.11}$$

$$E = 0.87eV - 0.14eV = \underline{0.73eV} \tag{4.12}$$

using the value of δ

$$E = \frac{1.71kT_M^2}{\delta} \tag{4.13}$$

$$E = \frac{1.71 * 8.617 * 10^{-5} * (398.09)^2}{29.01} \tag{4.14}$$

$$E = \underline{0.8eV} \tag{4.15}$$

using the value of ω

$$E = \frac{3.54kT_M^2}{\omega} - 2kT_M \tag{4.16}$$

$$E = \frac{3.54 * 8.617 * 10^{-5}(398.09)^2}{57.5} - 2 * 8.617 * 10^{-5} * 398.09 \tag{4.17}$$

$$E = 0.84eV - 0.07eV = \underline{0.77eV} \tag{4.18}$$

Peak 3

using the value of τ

$$E = \frac{1.81kT_M^2}{\tau} - 2(2kT_M) \tag{4.19}$$

$$E = \frac{1.81 * 8.617 * 10^{-5}(433.37)^2}{51.32} - 2(2 * 8.617 * 10^{-5} * 433.37) \tag{4.20}$$

$$E = 0.57eV - 0.15eV = \underline{0.42eV} \tag{4.21}$$

using the value of δ

$$E = \frac{1.71kT_M^2}{\delta} \tag{4.22}$$

$$E = \frac{1.71 * 8.617 * 10^{-5} * (433.37)^2}{51.49} \tag{4.23}$$

$$E = \underline{0.54eV} \tag{4.24}$$

using the value of ω

$$E = \frac{3.54kT_M^2}{\omega} - 2kT_M \tag{4.25}$$

$$E = \frac{3.54 * 8.617 * 10^{-5}(433.37)^2}{103.26} - 2 * 8.617 * 10^{-5} * 433.37 \tag{4.26}$$

$$E = 0.55eV - 0.07eV = \underline{0.48eV} \tag{4.27}$$

Peak 4

using the value of τ

$$E = \frac{1.81kT_M^2}{\tau} - 2(2kT_M) \tag{4.28}$$

$$E = \frac{1.81 * 8.617 * 10^{-5} * (546.53)^2}{103.33} - 2(2kT_M) \tag{4.29}$$

$$E = 0.45eV - 0.19eV = \underline{0.26eV} \tag{4.30}$$

using the value of δ

$$E = \frac{1.71kT_M^2}{\delta} \tag{4.31}$$

$$E = \frac{1.71 * 8.617 * 10^{-5} * (546.53)^2}{102.97} \tag{4.32}$$

$$E = \underline{0.43eV} \tag{4.33}$$

using the value of ω

$$E = \frac{3.54kT_M^2}{\omega} - 2kT_M \tag{4.34}$$

$$E = \frac{3.54 * 8.617 * 10^{-5}(546.53)^2}{\omega} - 2 * 8.617 * 10^{-5} * 546.53 \tag{4.35}$$

$$E = 0.44eV - 0.09eV = \underline{0.35eV} \tag{4.36}$$

4.2.2 Frequency Factor(s)

Frequency factor(s) was calculated by Kitis et al equation[25] of second order peak with the values of activation energy(E) calculated above using the values of τ, δ and ω for each peaks as following:

Peak 1

For E=0.91eV , $T_M = 371.9K$**,** $\beta = 1Ks^{-1}$ **and** $k = 8.617 * 10^{-5}eVK^{-1}$

$$s = \frac{\beta E}{kT_M^2(1 + \frac{2kT_M}{E})} \exp(\frac{E}{kT_M}) \tag{4.37}$$

$$s = \underline{1.57 * 10^{11} s^{-1}} \tag{4.38}$$

For E=0.96 eV , $T_M = 371.9K$**,** $\beta = 1Ks^{-1}$ **and** $k = 8.617 * 10^{-5} eVK^{-1}$

$$s = \underline{8.07 * 10^{11} s^{-1}} \tag{4.39}$$

For E=0.95 eV , $T_M = 371.9K$**,** $\beta = 1Ks^{-1}$ **and** $k = 8.617 * 10^{-5} eVK^{-1}$

$$s = \underline{9.3 * 10^{12} s^{-1}} \tag{4.40}$$

Peak 2

For E=0.73 eV , $T_M = 398.09K$**,** $\beta = 1Ks^{-1}$ **and** $k = 8.617 * 10^{-5} eVK^{-1}$

$$s = \frac{\beta E}{kT_M^2(1 + \frac{2kT_M}{E})} \exp(\frac{E}{kT_M}) \tag{4.41}$$

$$s = \underline{1.03 * 10^{8} s^{-1}} \tag{4.42}$$

For E=0.8 eV , $T_M = 398.09K$**,** $\beta = 1Ks^{-1}$ **and** $k = 8.617 * 10^{-5} eVK^{-1}$

$$s = \underline{8.3 * 10^{8} s^{-1}} \tag{4.43}$$

For E=0.77 eV , $T_M = 398.09K$**,** $\beta = 1Ks^{-1}$ **and** $k = 8.617 * 10^{-5} eVK^{-1}$

$$s = \underline{3.5 * 10^{8} s^{-1}} \tag{4.44}$$

Peak 3

For E=0.42 eV , $T_M = 433.37K$**,** $\beta = 1Ks^{-1}$ **and** $k = 8.617 * 10^{-5} eVK^{-1}$

$$s = \frac{\beta E}{kT_M^2(1 + \frac{2kT_M}{E})} \exp(\frac{E}{kT_M}) \tag{4.45}$$

$$s = \underline{1.869 * 10^4 s^{-1}} \tag{4.46}$$

For E=0.54 eV , $T_M = 433.37K$**,** $\beta = 1Ks^{-1}$ **and** $k = 8.617 * 10^{-5}eVK^{-1}$

$$s = \frac{\beta E}{kT_M^2(1 + \frac{2kT_M}{E})} \exp(\frac{E}{kT_M}) \tag{4.47}$$

$$s = \underline{1.657 * 10^4 s^{-1}} \tag{4.48}$$

For E=0.48 eV , $T_M = 433.37K$**,** $\beta = 1Ks^{-1}$ **and** $k = 8.617 * 10^{-5}eVK^{-1}$

$$s = \frac{\beta E}{kT_M^2(1 + \frac{2kT_M}{E})} \exp(\frac{E}{kT_M}) \tag{4.49}$$

$$s = \underline{1.07 * 10^4 s^{-1}} \tag{4.50}$$

Peak 4

For E=0.26 eV , $T_M = 546.53K$**,** $\beta = 1Ks^{-1}$ **and** $k = 8.617 * 10^{-5}eVK^{-1}$

$$s = \frac{\beta E}{kT_M^2(1 + \frac{2kT_M}{E})} \exp(\frac{E}{kT_M}) \tag{4.51}$$

$$s = \underline{1.7 * 10^1 s^{-1}} \tag{4.52}$$

For E=0.43 eV , $T_M = 546.53K$**,** $\beta = 1Ks^{-1}$ **and** $k = 8.617 * 10^{-5}eVK^{-1}$

$$s = \frac{\beta E}{kT_M^2(1 + \frac{2kT_M}{E})} \exp(\frac{E}{kT_M}) \tag{4.53}$$

$$s = \underline{1.31 * 10^2 s^{-1}} \tag{4.54}$$

For E=0.35 eV , $T_M = 546.53K$**,** $\beta = 1Ks^{-1}$ **and** $k = 8.617 * 10^{-5} eVK^{-1}$

$$s = \frac{\beta E}{kT_M^2(1 + \frac{2kT_M}{E})} \exp(\frac{E}{kT_M}) \tag{4.55}$$

$$s = \underline{1.9 * 10^1 s^{-1}} \tag{4.56}$$

4.3 Analysis of Glow Peaks Using Mathematica

By using the determined value of activation energy and frequency factor, also the total trap concentration(N=10^{10}), initial concentration of electron($n_o = 1 * 10^{10}$) and Boltzmann constant($k = 8.617 * 10^{-}5$) the graph of concentration of electron(n(T)) and TL intensity versus temperature were plotted on ***Mathemathica*** using the command **NDSolve** used to perform the numerical integration of the differential equation, and stores the result of the numerical integration as the parameter **sol** (which stands for the solution of the differential equation) for the deconvoluted peaks.

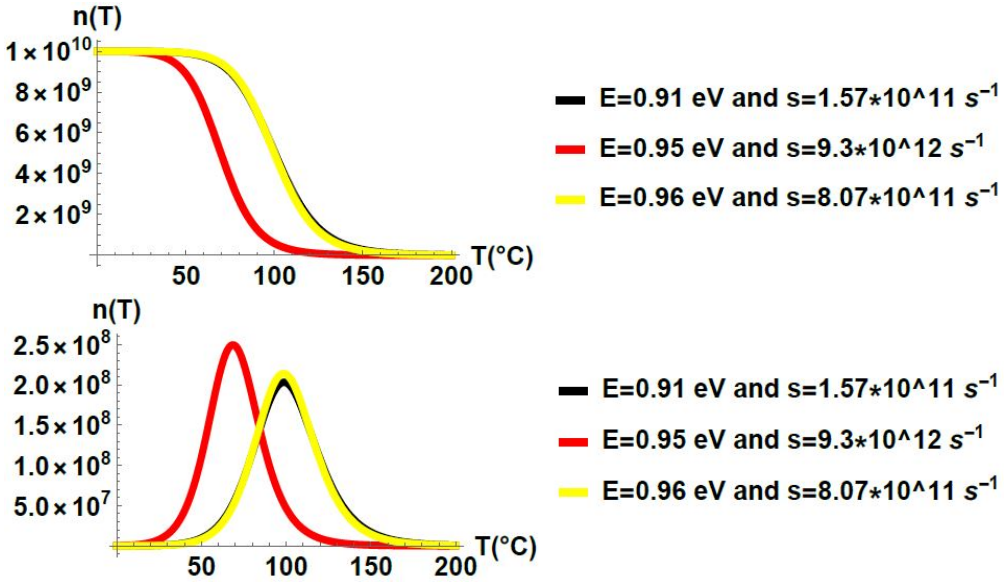

Figure 4.3: Concentration of electron and TL intensity of peak-1

The result of fig 4.3 shows that the sample was heated from 0°Cto 200°C, from 0°Cto 30°Cthere was no electron trap to the conduction band(CB) for E=0.91 eV and s=$1.57 * 10^{11} s^{-1}$ and from 0°Cto 50°Cfor E=0.95 eV and s=$9.3 * 10^{12} s^{-1}$ and E=0.96eV and s=$8.07 * 10^{11} s^{-1}$, because, the temperature was not enough to eject it. But, at temperature 40°Cand 60°Cthere was an electron trapped to CB and the concentration of electrons in the conduction band increases up to a maximum temperature at which the maximum intensity was observed, of approximately 70°C, 100°Cand 100°Cfor the values of E=0.91 eV and s=$1.57 * 10^{11} s^{-1}$, E=0.95 eV and s=$9.3 * 10^{12} s^{-1}$, and E=0.96eV and s=$8.07 * 10^{11} s^{-1}$ respectively. At 200°Call electrons were excited to CB. From the graph of TL versus temperature of the value of maximum temperature(T_M) of E=0.91 eV and s=$1.57 * 10^{11} s^{-1}$ and E=0.96eV and s=$8.07 * 10^{11} s^{-1}$ was very close to the maximum temperature of the experimental glow curve peak-1. But, T_M of the peak with the value E=0.95 eV and s=$9.3 * 10^{12} s^{-1}$ was far from its experimental value. The curve with the value E=0.95 eV and s=$9.3 * 10^{12} s^{-1}$ shifts to lower temperature because it has higher order of frequency(10^{12}) than the others and the peak with high order of frequency shifts to lower temperature with increase in height and decrease in width. A trapping center with a high frequency factor needs less energy to free a charge carrier[5]. Curves with E=0.91 eV and s=$1.57 * 10^{11} s^{-1}$ and E=0.96eV and s=$8.07 * 10^{11} s^{-1}$ has lower order of frequency(10^{11}) than the other and the peak with lower order of frequency factor shift to higher temperature with decrease in height and increase in width, because the trapping center with lower frequency factor needs high energy to free charge carrier[5].

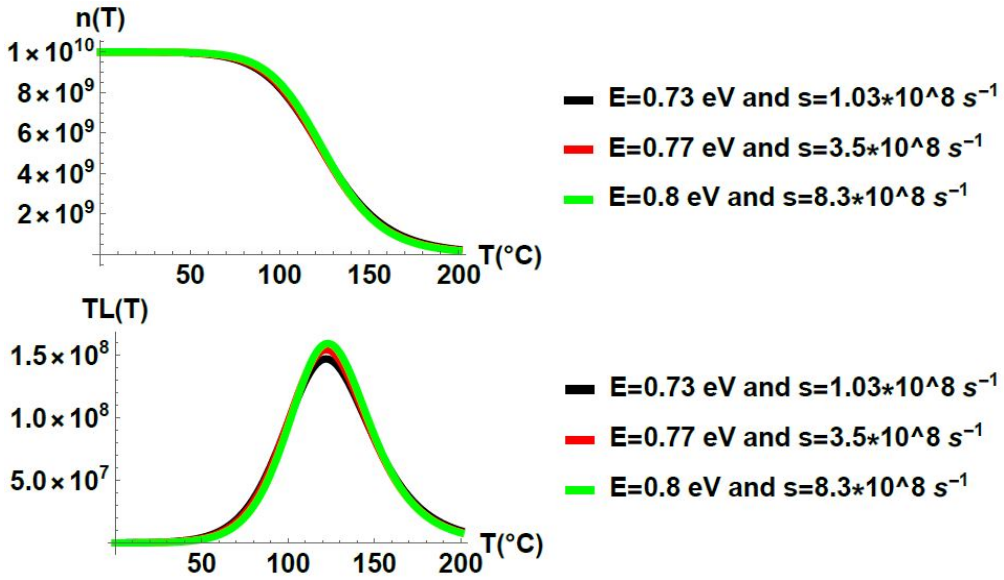

Figure 4.4: Concentration of electron and TL intensity of peak-2

Fig 4.4 shows that as peak-1 the sample was heated from 0°Cto 200°C, from 0°Cto 50°Cthere was no electron trapped to CB because the temperature was not enough to eject electron from the trap. But, at 60°Cthere was an electron trapped to CB and the concentration of electron in the CB increases up to T_M at which the maximum TL intensity observed approximately between 120°Cand 130°Cfor the three values of E and s. This value of maximum temperature coincides with the experimental value of maximum temperature of peak-2. From TL intensity curve we observed that as frequency factor increases the height of the peaks were increased and width decrease, as activation energy increases there was little peak shift toward higher temperature.

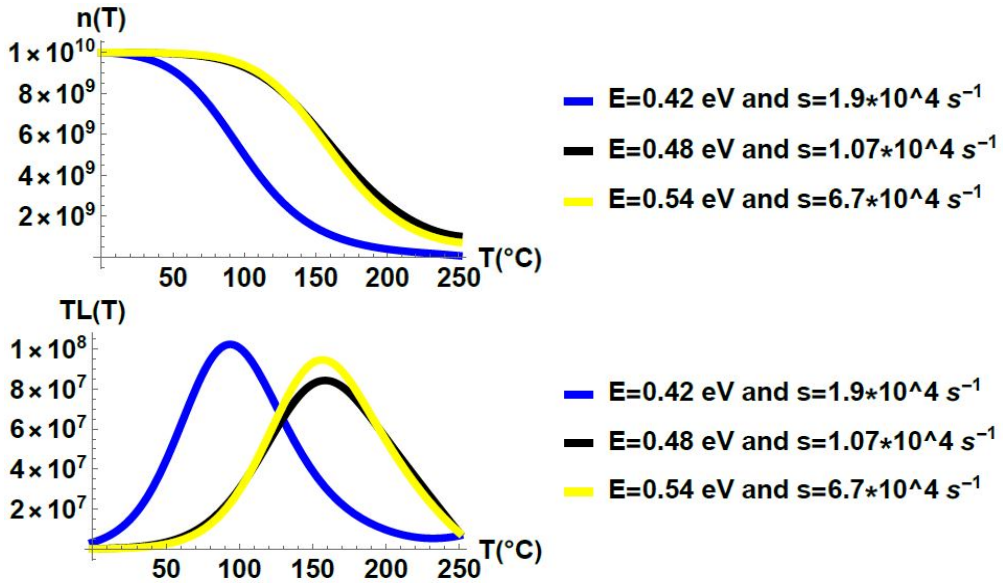

Figure 4.5: Concentration of electron and TL intensity of peak-3

The result of the above fig 4.5 shows that the sample was heated from 0°Cto 200°C, from 0°Cto 10°Cthere was no electron trapped to CB for E=0.42eV and $s = 1.9 * 10^4\ s^{-1}$, from 0°Cto 50°Cthere was no electron trapped to CB for E=0.48 eV and $s = 1.07 * 10^4\ s^{-1}$ and E=0.54 eV and $s = 6.7 * 10^4 s^{-1}$. But, for the value E= 0.42 eV and $s = 1.9 * 10^4\ s^{-1}$ at 20°Cand for E=0.48 eV and $s = 1.07 * 10^4\ s^{-1}$ and E=0.54 eV and $s = 6.7 * 10^4 s^{-1}$ at 80°Cthere was the electron trapped to the CB and the concentration of electron in the CB increases up to a maximum temperature at which maximum TL intensity was observed of approximately 90°Cfor E=0.42 eV and s=1.9*$10^4\ s^{-1}$, 160°Cfor E=0.48eV and $s = 1.07 * 10^4\ s^{-1}$ and E=0.54eV and $s = 6.7 * 10^4\ s^{-1}$ approximately. Even though the sample was heated from 0°Cto 200°C, but there was the excitation of electron to the CB and TL intensity above 200°C. The value of maximum temperature of E=0.48eV and $s = 1.07 * 10^4\ s^{-1}$ and E=0.54eV and $s = 6.7 * 10^4\ s^{-1}$ were very close to its experimental value of T_M, but T_M of E= 0.42 eV and $s = 1.9 * 10^4\ s^{-1}$ was far from the experimental value of T_M of peak-3. The curve with the value of E= 0.42 eV and $s = 1.9 * 10^4\ s^{-1}$ shifted to lower temperature because it has lower activation energy than the others. For lower E value(shallower traps) less energy(lower energy) is needed to release the charge carrier[5].

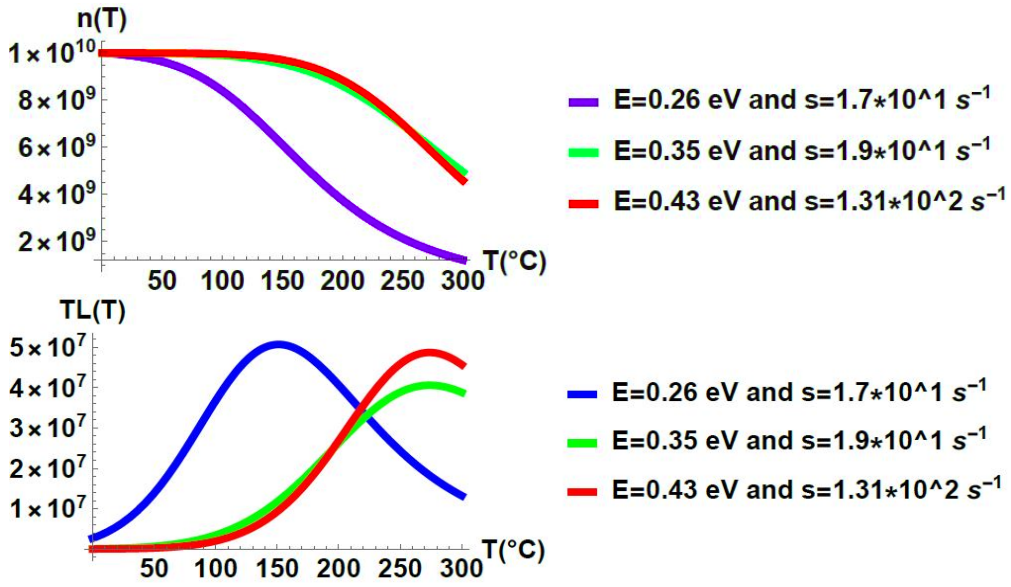

Figure 4.6: Concentration of electron and TL intensity of peak-4

Fig 4.6 shows that the sample was heated from 0°Cto 300°C, at 0°Cthere was electron trapped to CB for E=0.26 eV and $s = 1.7 * 10^1 s^{-1}$, from 0°Cto 100°Cthere was no electron trapped to CB for E=0.35 eV and $1.9 * 10^1 s^{-1}$, and E=0.43 eV and $s = 1.31 * 10^2 s^{-1}$ because the temperature was not enough to eject it. The concentration of electron in the CB increase up to the maximum temperature at which maximum intensity observed approximately 150°Cand between 270°Cand 280°Cfor E=0.26 eV and $s = 1.7 * 10^1 s^{-1}$, and E=0.35 eV and $1.9 * 10^1 s^{-1}$, E=0.43 eV and $s = 1.31 * 10^2 s^{-1}$ approximately. Similar to peak-3, there was excitation of electrons to the CB and TL intensity produced above 300°Cfor E=0.35 eV and $1.9 * 10^1 s^{-1}$, and E=0.43 eV and $s = 1.31 * 10^2 s^{-1}$, and for E=0.26 eV and $s = 1.7 * 10^1 s^{-1}$ there was no excited electron to CB but there was TL intensity above 300°C. The T_M values of the curve(with color red and green) were very close to the experimental value of T_M of peak-4, while the other curve(the blue one) was not. Curves with E=0.26 eV and $s = 1.7 * 10^1 s^{-1}$ were shifted to lower temperature because it have lower value of activation energy than the others. For lower value(shallower traps) less energy(lower temperature) is needed to free charge carrier[5].

Table 4.3: Summary of activation energy and frequency factor

Peaks	E(eV)			s(s^{-1})		
	Using τ	Using δ	Using ω	Using τ	Using δ	Using ω
Peak 1	0.91	0.96	0.95	1.57*10^{11}	8.07*10^{11}	9.3*10^{12}
Peak 2	0.73	0.8	0.77	1.03*10^{8}	8.3*10^{8}	3.5*10^{8}
Peak 3	0.42	0.54	0.48	1.869*10^{4}	1.657*10^{4}	1.07*10^{4}
Peak 4	0.26	0.43	0.35	1.7*10^{1}	1.31*10^{2}	1.9$10^{1}$

5

Conclusion

In this work, we studied the TL glow curve deconvolution analysis of Calcium Magnesium Silicate nanophosphor using the concept of one trap one recombination center(OTOR) model. The glow curve was plotted and analyzed on Origin with the experimental data of host material. Four peaks were deconvoluted from the curve of host material and for each peaks activation energy and frequency factor were determined using peak shape method expression of second order kinetics, because the calculated value of μ was very close to 0.52 which is for second order. Summary of the determined value of E and s were recorded in table 4.3. With the value of activation energy(E), frequency factor(s), total concentration of trap(N=$10^{10}m^{-3}$), initial concentration of electron($n_o = 1 * 10^{10}$) and Boltzmann constant(k=$8.617 * 10^{-5}eVK^{-1}$), the graph of concentration of electron and TL intensity versus temperature were plotted for each peaks on the mathematica. From these peaks we observed that the values of maximum temperature(T_M) theoretically were very close to the values of their T_M experimentally and also their intensity were shifted as the following:

- For peak-1 TL intensity of the curve with value E=0.95 eV and s=$9.3*10^{12}s^{-1}$ shifted to lower temperature due to its higher order of frequency factor.
- For peak-2 TL intensity curve increase in height and decrease in width as frequency factor increases and as activation energy increase there was little peak shift toward higher temperature.
- For peak-3 TL intensity of the curve with value E=0.42 eV and s=$1.9 * 10^4 s^{-1}$ shifts to lower temperature due to its lower activation energy.
- TL intensity of peak-4 of the curve with value E=0.26 eV and s=$1.7 * 10^1 s^{-1}$ shifted

toward lower temperature due to its lower activation energy.

Bibliography

[1] Akat'eva LV, Kozyukhin SA. Luminophores based on synthetic calcium silicates. Theoretical Foundations of Chemical Engineering. 2015 Sep;49(5):706-13.

[2] Alam S, Bauk S. The Effect of the Activation Energy, Frequency Factor and the Initial Concentration of Filled Traps on the TL Glow Curves of Thermoluminescence. Adv. Studies Theor. Phys. 2010;4:665-78.

[3] Bhattacharyya S, Majumdar PS. An Overview on Peak Shape Method for Thermoluminescence Glow Curve Analysis: Application on Tremolite and Actinolite Glow Peaks. Emerging Synthesis Techniques for Luminescent Materials. 2018:26-52.

[4] Basun S, Imbusch GF, Jia DD, Yen WM. The analysis of thermoluminescence glow curves. Journal of Luminescence. 2003 Aug 1;104(4):283-94.

[5] Bos AJ. Theory of thermoluminescence. Radiation measurements. 2006 Dec 1;41:S45-56.

[6] Chandrakar P, Baghel RN, Bisen DP, Chandra BP. Characterization and luminescence properties of CaMgSi2O6: Eu2+ blue phosphor. Luminescence. 2015 Nov;30(7):1034-40.

[7] Chen R. and Kirsh Y., Analysis of Thermally Stimulated Processes, pergamon press, 1981

[8] Chen R, Pagonis V, Lawless JL. Evaluated thermoluminescence trapping parameters–What do they really mean?. Radiation Measurements. 2016 Aug 1;91:21-7.

[9] Chen R, Pagonis V. On the quasi-equilibrium assumptions in the theory of thermoluminescence (TL). Journal of luminescence. 2013 Nov 1;143:734-40.

[10] Chen, Xianchun, Xiaoming Liao, Zhongbing Huang, Panli You, Chun Chen, Yunqing Kang, and Guangfu Yin. "Synthesis and characterization of novel multiphase bioactive glass-ceramics in the CaO-MgO-SiO2 system." no. 1 (2010): 194-202.

[11] Clabau F, Rocquefelte X, Jobic S, Deniard P, Whangbo MH, Garcia A, Le Mercier T. Mechanism of phosphorescence appropriate for the long-lasting phosphors Eu2+-doped SrAl2O4 with codopants Dy3+ and B3+. Chemistry of materials. 2005 Jul 26;17(15):3904-12.

[12] Furetta C. Handbook of thermoluminescence. World Scientific; 2010.

[13] Furetta C, Kitis G. Models in thermoluminescence. Journal of materials science. 2004 Apr;39(7):2277-94.

[14] Furetta C. Models and methods in thermoluminescence.2005

[15] Fu Z, Zhou S, Zhang S. Study on optical properties of rare-earth ions in nanocrystalline monoclinic SrAl2O4: Ln (Ln= Ce3+, Pr3+, Tb3+). The Journal of Physical Chemistry B. 2005 Aug 4;109(30):14396-400.

[16] G.Kitis, J. Papadopoulos, S. Charalambousn and J.N. Tuyn. The influence of heating rate on the response and trapping parameters of $\alpha - Al_2O_3$: C. Radiat. Prot. Dosim., 55:183–190, 1994.

[17] Horowitz YS, Yossian D. Computerised glow curve deconvolution: application to thermoluminescence dosimetry. Radiation Protection Dosimetry. 1995 Jun 1;60(1):3-
.

[18] Iwata NY, Lee GH, Tsunakawa S, Tokuoka Y, Kawashima N. Preparation of diopside with apatite-forming ability by sol–gel process using metal alkoxide and metal salts. Colloids and Surfaces B: Biointerfaces. 2004 Jan 1;33(1):1-6.

[19] J.B. Pendry, A.J. Holden, W.J. Stewart, and I. Youngs, Extremely low frequency plasmons in metallic meso structures, Phys. Rev. Lett. 76(25), 4773 (1996).

[20] Kirsh Y. Kinetic analysis of thermoluminescence. physica status solidi (a). 1992 Jan 16;129(1):15-48.

[21] Kitis G. TL glow-curve deconvolution functions for various kinetic orders and continuous trap distribution: Acceptance criteria for E and s values. Journal of Radioanalytical and Nuclear Chemistry. 2001 Mar 18;247(3):697-703.

[22] Kunimoto T, Honma T, Ohmi K, Okubo S, Ohta H. Detailed impurity phase investigation by X-ray absorption fine structure and electron spin resonance analyses in synthesis of CaMgSi2O6: eu phosphor. Japanese Journal of Applied Physics. 2013 Mar 29;52(4R):042402.

[23] McKeever SW. Thermoluminescence of solids. Cambridge University Press; 1988 Oct 27.

[24] Murthy KV, Virk HS. Luminescence phenomena: an introduction. InDefect and diffusion fórum 2014 (Vol. 347, pp. 1-34). Trans Tech Publications Ltd.

[25] Pagonis V, Kitis G, Furetta C. Numerical and practical exercises in thermoluminescence. Springer Science Business Media; 2006 Jan 4.

[26] R. Chen and S.W.S. McKeever. Theory of Thermoluminescence and Related Phenomena. World Scientific Publishing, 1997.

[27] Randall JT, Wilkins MH. Phosphorescence and electron traps-I. The study of trap distributions. Proceedings of the Royal Society of London. Series A. Mathematical and Physical Sciences. 1945 Nov 6;184(999):365-89.

[28] Razavi M, Fathi M, Savabi O, Razavi SM, Beni BH, Vashaee D, Tayebi L. Surface modification of magnesium alloy implants by nanostructured bredigite coating. Materials Letters. 2013 Dec 15;113:174-8.

[29] Razavi M, Fathi M, Savabi O, Vashaee D, Tayebi L. In vivo study of nanostructured akermanite/PEO coating on biodegradable magnesium alloy for biomedical applications. Journal of Biomedical Materials Research Part A. 2015 May;103(5):1798-808.

[30] Srinath P, Azeem PA, Reddy KV, Chiranjeevi P, Bramanandam M, Rao RP. A novel cost-effective approach to fabricate diopside bioceramics: A promising ceramics for orthopedic applications. Advanced Powder Technology. 2021 Mar 1;32(3):875-84.

[31] S.W.S. McKeever, Thermoluminescence of Solids, Cambridge University Press, Cambridge, 1985.

[32] Yamamoto Y. Thermoluminescent materials. 1990.

[33] Yu X, Zhou C, He X, Peng Z, Yang SP. The influence of some processing conditions on luminescence of SrAl2O4: Eu2+ nanoparticles produced by combustion method. Materials Letters. 2004 Feb 1;58(6):1087-91.

Figure 5.1: Table of experimental data for host material

S/N	Temp(˚C)	Intensity	S/N	Temp(˚C)	Intensity	S/N	Temp(˚C)	Intensity
1	2.3	165.09	31	71.3	260.75	61	140.3	675.4
2	4.6	164.13	32	73.6	282.37	62	142.6	666.09
3	6.9	162.26	33	75.9	305.24	63	144.9	655.86
4	9.2	159.57	34	78.2	329.18	64	147.2	644.85
5	11.5	156.17	35	80.5	354.04	65	149.5	633.23
6	13.8	152.23	36	82.8	379.59	66	151.8	621.12
7	16.1	147.91	37	85.1	405.62	67	154.1	608.68
8	18.4	143.38	38	87.4	431.87	68	156.4	596
9	20.7	138.8	39	89.7	458.1	69	158.7	583.21
10	23	134.34	40	92	484.03	70	161	570.4
11	25.3	130.14	41	94.3	509.41	71	163.3	557.63
12	27.6	126.34	42	96.6	533.97	72	165.6	544.98
13	29.9	123.05	43	98.9	557.47	73	167.9	532.5
14	32.2	120.39	44	101.2	579.7	74	170.2	520.2
15	34.5	118.48	45	103.5	600.46	75	172.5	508.11
16	36.8	117.42	46	105.8	619.57	76	174.8	496.22
17	39.1	117.31	47	108.1	636.89	77	177.1	484.51
18	41.4	118.26	48	110.4	652.31	78	179.4	472.94
19	43.7	120.37	49	112.7	665.75	79	181.7	461.44
20	46	123.74	50	115	677.14	80	184	449.96
21	48.3	128.47	51	117.3	686.47	81	186.3	438.43
22	50.6	134.62	52	119.6	693.72	82	188.6	426.8
23	52.9	142.27	53	121.9	698.92	83	190.9	415.02
24	55.2	151.48	54	124.2	702.1	84	193.2	403.09
25	57.5	162.28	55	126.5	703.34	85	195.5	391.05
26	59.8	174.71	56	128.8	702.69	86	197.8	378.97
27	62.1	188.76	57	131.1	700.28	87	200.1	366.99
28	64.4	204.43	58	133.4	696.21	88	202.4	355.24
29	66.7	221.69	59	135.7	690.61	89	204.7	343.93
30	69	240.49	60	138	683.62	90	207	333.25

91	209.3	323.37	121	278.3	233.06	151	347.3	138.04
92	211.6	314.47	122	280.6	230	152	349.6	135.07
93	213.9	306.65	123	282.9	227.12	153	351.9	132.33
94	216.2	299.97	124	285.2	224.46	154	354.2	129.8
95	218.5	294.43	125	287.5	222.04	155	356.5	127.48
96	220.8	289.98	126	289.8	219.86	156	358.8	125.35
97	223.1	286.51	127	292.1	217.93	157	361.1	123.41
98	225.4	283.88	128	294.4	216.2	158	363.4	121.63
99	227.7	281.93	129	296.7	214.62	159	365.7	120.02
100	230	280.48	130	299	213.11	160	368	118.54
101	232.3	279.38	131	301.3	211.58	161	370.3	117.2
102	234.6	278.46	132	303.6	209.91	162	372.6	115.98
103	236.9	277.59	133	305.9	208.02	163	374.9	114.87
104	239.2	276.66	134	308.2	205.81	164	377.2	113.85
105	241.5	275.59	135	310.5	203.22	165	379.5	112.89
106	243.8	274.33	136	312.8	200.21	166	381.8	111.97
107	246.1	272.84	137	315.1	196.77	167	384.1	111.06
108	248.4	271.09	138	317.4	192.94	168	386.4	110.13
109	250.7	269.1	139	319.7	188.77	169	388.7	109.13
110	253	266.86	140	322	184.32	170	391	108.03
111	255.3	264.39	141	324.3	179.68	171	393.3	106.8
112	257.6	261.71	142	326.6	174.94	172	395.6	105.4
113	259.9	258.86	143	328.9	170.18	173	397.9	103.82
114	262.2	255.86	144	331.2	165.49	174	400.2	102.04
115	264.5	252.73	145	333.5	160.93	175	402.5	100.06
116	266.8	249.5	146	335.8	156.54	176	404.8	97.89
117	269.1	246.2	147	338.1	152.36	177	407.1	95.55
118	271.4	242.86	148	340.4	148.41	178	409.4	93.08
119	273.7	239.54	149	342.7	144.71	179	411.7	90.51
120	276	236.26	150	345	141.25	180	414	87.88

181	416.3	85.24
182	418.6	82.61
183	420.9	80.05
184	423.2	77.56
185	425.5	75.18
186	427.8	72.92
187	430.1	70.79
188	432.4	68.78
189	434.7	66.91
190	437	65.16
191	439.3	63.54
192	441.6	62.05
193	443.9	60.69
194	446.2	59.47
195	448.5	58.38
196	450.8	57.44
197	453.1	56.67
198	455.4	56.08
199	457.7	55.68
200	460	55.48